AGU PUBLICATIONS

Paleoceanography

RESEARCH ARTICLE
10.1002/2014PA002758

Key Points:
- Hydrogen index and $\delta^{13}C_{TOC}$ data are compared for three Toarcian sections
- The Toarcian negative CIE is exaggerated by changes in OM contribution
- The Toarcian CIE has an amplitude of 4‰ in marine OM

Supporting Information:
- Figures S1 and S2 and Table S1

Correspondence to:
G. Suan,
guillaume.suan@univ-lyon1.fr

Citation:
Suan, G., B. van de Schootbrugge, T. Adatte, J. Fiebig, and W. Oschmann (2015), Calibrating the magnitude of the Toarcian carbon cycle perturbation, *Paleoceanography*, *30*, 495–509, doi:10.1002/2014PA002758.

Received 18 NOV 2014
Accepted 8 APR 2015
Accepted article online 14 APR 2015
Published online 13 MAY 2015

Calibrating the magnitude of the Toarcian carbon cycle perturbation

Guillaume Suan[1,2], Bas van de Schootbrugge[3], Thierry Adatte[4], Jens Fiebig[2], and Wolfgang Oschmann[2]

[1]UMR CNRS 5276 LGLTPE, Université Lyon 1, École Normale Supérieure de Lyon, Villeurbanne Cedex, France, [2]Institute of Geosciences, Goethe University Frankfurt, Frankfurt am Main, Germany, [3]Institute of Earth Sciences, Utrecht University, Utrecht, Netherlands, [4]Institut des Sciences de la Terre, Université de Lausanne, Lausanne, Switzerland

Abstract Sedimentary rocks recording the Toarcian oceanic anoxic event (T-OAE) are marked by a negative carbon isotope excursion (CIE) reaching up to −7‰ and ranking among the largest known in the Phanerozoic. These records suggest a dramatic perturbation of the carbon cycle that has been linked to the transfer of juvenile carbon from the endogenic to the exogenic reservoirs. Nevertheless, the magnitude of the Toarcian CIE varies significantly from one substrate to another, hence complicating mass balance evaluation of the potential driving mechanisms. Here we show, using high-resolution, paired records of $\delta^{13}C_{total\ organic\ carbon\ (TOC)}$ and hydrogen index from the Denkingen core and Dotternhausen quarry (Germany), that the amplitude of the negative CIE in marine organic matter is considerably exaggerated by changes in organic matter sourcing. Our corrected 3–4‰ CIE implies a constant carbon isotope fractionation between organic and carbonate carbon across the T-OAE and may point to a prominent role of cyanobacteria as organic matter producers during the Early Jurassic. These results also suggest that the difference between inorganic and organic carbon isotope values in marine strata constitutes a poor proxy of pCO_2 levels across the T-OAE. Moreover, this corrected 3–4‰ CIE, together with evidence for >5°C seawater warming across the T-OAE, point to the input of >25,000 Gt C with much more ^{13}C-enriched signature than previously modeled. Our results thus allow reconciling inorganic and organic $\delta^{13}C$ records of the T-OAE and have important implications for the evaluation of their causal mechanisms.

1. Introduction

The Early Jurassic time, spanning 25 Ma of Earth history (201–175 Ma), was marked by repeated ocean deoxygenation and black shale deposition (the so-called *Schwarzer Jura*, "Black Jurassic," of the German literature), culminating in the Toarcian oceanic anoxic event (T-OAE). The widely distributed organic carbon-rich deposits of this age [*Jenkyns*, 1988] bear evidence for pronounced excursions in carbon, osmium, nitrogen, oxygen, calcium, and sulfur isotopic systems [*Jenkyns et al*., 2001; *Cohen et al*., 2004; *Suan et al*., 2010; *Gill et al*., 2011; *Hesselbo and Pieńkowski*, 2011; *Brazier et al*., 2015]. The T-OAE is notably marked by one of the largest negative carbon isotope excursions (CIE) of the Mesozoic, which has been attributed to the massive release of isotopically light carbon to the oceanic and atmospheric reservoirs [*Hesselbo et al*., 2000; *Kemp et al*., 2005; *Beerling and Brentnall*, 2007; *Hesselbo et al*., 2007].

The Toarcian negative CIE spans the boundary between the *tenuicostatum* and *falciferum* ammonite zones (or their equivalents) in European successions, and its duration has been estimated as between 300 and 900 kyr [*Suan et al*., 2008b; *Boulila et al*., 2014]. The negative CIE and the following positive CIE rebound seen in the upper half of the *falciferum* zone in several successions [*Jenkyns*, 1988, 2010] are often considered as better time markers for the T-OAE than the organic-rich strata. Indeed, if one considers the lower Toarcian negative CIE as reflecting global and synchronous changes in carbon cycling, the lower Toarcian organic-rich strata, as with many organic-rich deposits associated with other OAEs, appear to be slightly to highly diachronous [*Jenkyns*, 2010; *Hermoso et al*., 2013; *Suan et al*., 2013; *van de Schootbrugge et al*., 2013]. In NW Europe and N Siberia, the organic-rich strata occur stratigraphically both within and well above the CIE (up to the top of the *bifrons* ammonite zone) [*Röhl et al*., 2001; *Suan et al*., 2011; *Hermoso et al*., 2013], whereas in S Europe, when present, they are generally bound to strata recording the CIE [*Sabatino et al*., 2009; *Kafousia et al*., 2011]. In most known successions, however, strata recording the negative CIE exhibit dramatic changes in geochemical, sedimentological, and micropaleontological composition [*Hesselbo et al*., 2007; *Mattioli et al*., 2009; *Hermoso et al*., 2012, 2013; *Kemp and Izumi*, 2014], suggesting that the carbon cycle perturbation was intimately linked with profound climatic and oceanographic disturbances.

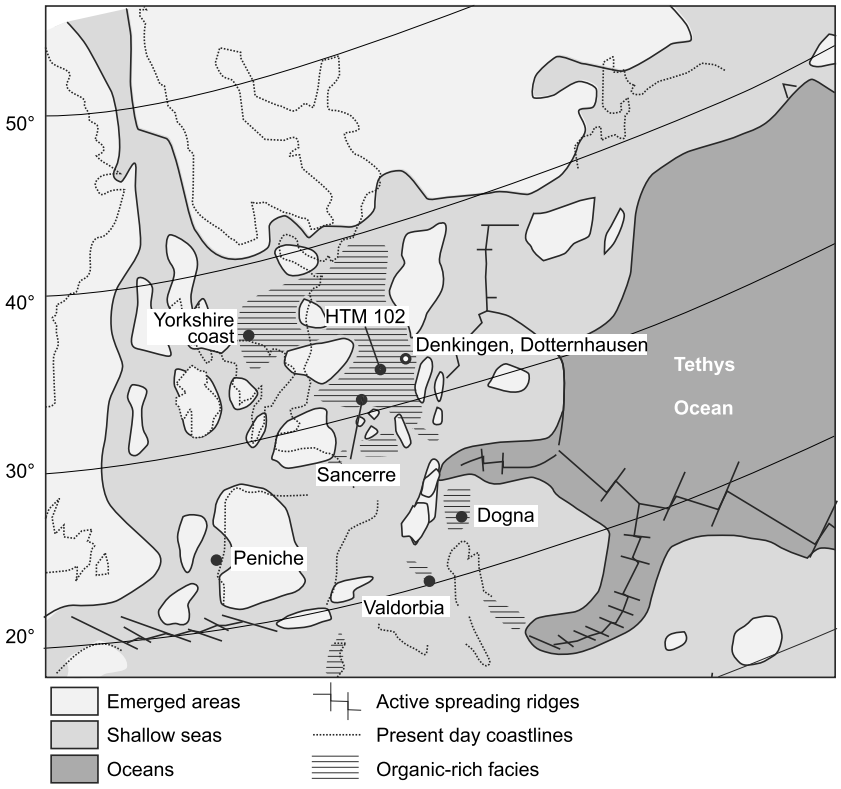

Figure 1. Paleogeographic location of studied sites (white circle) and previous studied sites (black circles) as discussed in the text. The paleogeographic reconstruction is modified from *Mattioli et al.* [2008]. The distribution of organic-rich facies is modified from *Baudin et al.* [1990].

Proposed sources of light carbon input that may have caused the Toarcian negative CIE include pulses of methane hydrate dissociation [*Kemp et al.*, 2005; *Cohen et al.*, 2007], thermogenic methane emissions from the intrusive eruption of the Karoo-Ferrar province [*Svensen et al.*, 2007], or the local recycling of remineralized carbon into superficial waters in restricted basin [*Küspert*, 1982; *Sælen et al.*, 2000; *Röhl et al.*, 2001; *van de Schootbrugge et al.*, 2005]. All these hypotheses are not mutually exclusive, and it appears likely that several mechanisms played in concert to produce the isotopic records. There is, however, currently no consensus about the relative importance of these various mechanisms.

A central issue to this debate is the extreme variability in magnitude (between −2 and −8‰) and shape of the inorganic and organic $\delta^{13}C$ records spanning the T-OAE [*van de Schootbrugge et al.*, 2005; *van Breugel et al.*, 2006; *Hesselbo et al.*, 2007; *French et al.*, 2014]. These discrepancies between organic and inorganic C-isotope records [*van de Schootbrugge et al.*, 2005; *Hesselbo et al.*, 2007] result in uncertainties about the possible amount of carbon released to the atmosphere during the Toarcian OAE, hampering attempts to faithfully model biogeochemical cycles governing this critical interval of Earth history. Crucially, most of the T-OAE $\delta^{13}C$ records are based on analyses of bulk organic matter (OM), which represents a complex admixture of allochthonous and autochthonous sources with potentially very variable $\delta^{13}C$ signatures [*Freeman and Hayes*, 1992; *Freeman*, 2001; *Sluijs and Dickens*, 2012]. For instance, Toarcian algal-rich sediment samples are 3–4‰ more depleted in ^{13}C than coeval fossilized wood in the successions of the Yorkshire Coast (UK) and Argentina [*Sælen et al.*, 2000; *Hesselbo et al.*, 2007; *Al-Suwaidi et al.*, 2010], suggesting that changes in OM source may exert a substantial influence on the $\delta^{13}C_{TOC}$ [*Littler et al.*, 2010; *van de Schootbrugge et al.*, 2013]. Unfortunately, the effects of changing OM sourcing on $\delta^{13}C_{TOC}$ during the T-OAE have seldom been explored and therefore remain poorly understood. Here we explore these effects using new and previously published, high-resolution carbon isotope and Rock-Eval pyrolysis data from biostratigraphically well-dated marine successions spanning the T-OAE from SW Germany and NE England.

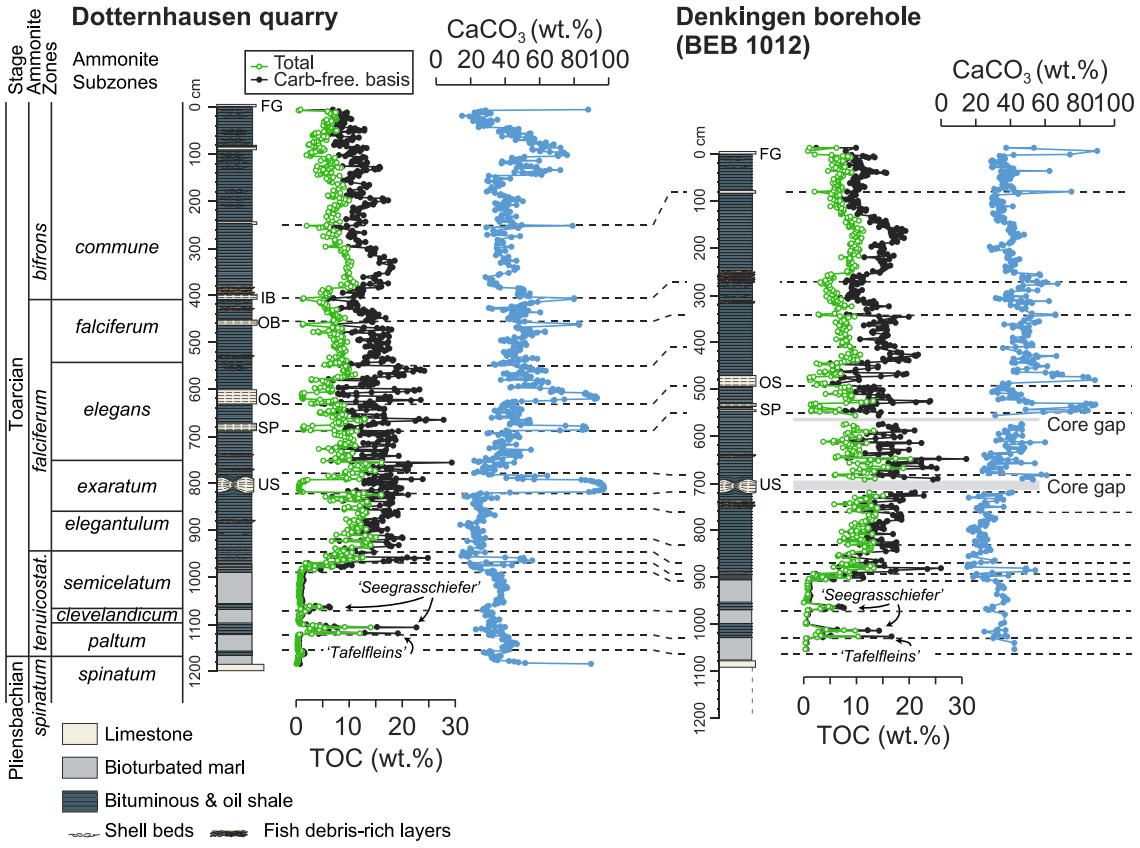

Figure 2. Correlation between the Pliensbachian-Toarcian successions of Dotternhausen and Denkingen borehole (SW Germany). Lithostratigraphy is from *Röhl et al.* [2001]. Abbreviations: U.S. = Unterer Stein; SP = Steinplatte; OB = Oberer Stein; OS = Oberer Bank; IB = Inoceramen Bank; FG = Fucoiden-Grenzbank; TOC = total organic carbon; *tenuicostat.* = *tenuicostatum*; and Carb-free basis = carbonate-free basis.

2. Samples

The studied material derives from the Denkingen BEB 1012 borehole drilled in 1978 in SW Germany (Figure 1) at 20 km SSW of the section exposed in Dotternhausen quarry [*Röhl et al.*, 2001]. The samples from Dotternhausen were originally collected from a temporary excavation for the upper part of the succession (*falciferum* and *bifrons* ammonite zones) and from an ~2.4 m core for the *spinatum* and *tenuicostatum* ammonite zones [*Schmid-Röhl*, 1999]. The correlation between Denkingen and Dotternhausen is crucial as the succession at Dotternhausen benefits from a biostratigraphic framework based on both ammonites [*Riegraf et al.*, 1984] and nannofossils [*Mattioli et al.*, 2008] and constitutes one of the best studied lower Toarcian successions documented so far [*Röhl et al.*, 2001; *Frimmel et al.*, 2004; *Schwark and Frimmel*, 2004; *Röhl and Schmid-Röhl*, 2005]. Excellent correlations between Denkingen and Dotternhausen can be achieved using a number of marker beds that occur throughout SW Germany [*Riegraf et al.*, 1984] and the abundant geochemical data available for both sites (Figure 2). These correlations provide a high-resolution biostratigraphical framework for the Denkingen borehole (Figure 2). Strongly bioturbated marls with diversified benthic assemblages characterize the major part of the *tenuicostatum* zone in both sections (Figure 2), while laminated bituminous and oil shales mostly devoid of benthic fauna dominate from the upper part of the *tenuicostatum* zone to the base of the *bifrons* zone. At both sites, the organic-rich interval contains several horizons rich in bivalves and fish debris (Figure 2).

3. Methods

Samples were collected for geochemical analyses at a 2 cm average spacing in Denkingen. The bulk carbonate carbon and oxygen isotope composition ($\delta^{13}C_{carb}$ and $\delta^{18}O_{carb}$) of 257 samples and the bulk organic carbon isotope composition ($\delta^{13}C_{TOC}$) of 148 samples were measured. The $\delta^{13}C_{carb}$ and $\delta^{18}O_{carb}$ ratios were

determined by analyzing 50 to 100 μg of oven-dried, bulk sediment powder with a Gas Bench II (Thermoquest) connected to the continuous flow inlet system of a MAT 253 mass spectrometer at the Institute of Geosciences (Goethe University Frankfurt). An internal standard, calibrated against NBS18 and NBS19, was run along with the samples. Internal precision was better than 0.05‰ for $\delta^{13}C_{carb}$ and 0.1‰ for $\delta^{18}O_{carb}$.

The $\delta^{13}C_{TOC}$ ratios along the Denkingen core were determined by analyzing 0.3 to 12 mg of decarbonated sediment powder with a Thermo Fisher Flash Elemental Analyzer 1112 connected to the continuous flow inlet system of a MAT 253 isotope ratio mass spectrometer (elemental analysis–isotope ratio mass spectrometry (EA-IRMS)) at the Institute of Geosciences (Goethe University Frankfurt). Prior to analysis, samples were decarbonated using excess 1 M HCl for 48 h in a sand bath at 50°C, rinsed with deionized water, and centrifuged until neutrality was reached. Analytical precision and accuracy were monitored by replicate analyses of U.S. Geological Survey 24 graphite standard. The reproducibility was better than 0.1‰. The $\delta^{13}C_{TOC}$ ratios for Dotternhausen were obtained on decarbonated samples using a Heraeus CHN-O-rapid elemental analyzer connected to a Finnigan MAT Delta-S mass spectrometer at the University of Köln [*Frimmel*, 2003].

Information on the type and thermal maturity of the bulk organic matter at Denkingen was obtained by Rock-Eval pyrolysis using a Rock-Eval 6 device at the Institut des Sciences de la Terre (Université de Lausanne) on decarbonated samples under standard conditions [*Behar et al*., 2001]. The TOC, hydrogen index (HI, mg HC g^{-1} TOC), oxygen index (OI, mg CO_2 g^{-1} TOC), and T_{max} (°C) were determined (Figure 3). Rock-Eval pyrolysis data for Dotternhausen were obtained by *Frimmel et al*. [2004] at the University of Köln using a Rock-Eval II *plus* device. The relative errors on HI measurements of source rock samples using this device are slightly higher (5% of the measured value) than those obtained using the Rock-Eval 6 apparatus (1.5% of the measured value) [*Spiro*, 1991; *Behar et al*., 2001].

Total organic carbon (TOC, in wt.%) contents at Denkingen were also determined using the EA peak areas obtained during $\delta^{13}C_{TOC}$ measurements. The TOC data obtained using the $\delta^{13}C_{TOC}$ measurements were compared to that obtained by combustion with a vario EL elemental analyzer (Elementar) and Rock-Eval pyrolysis. There is an excellent agreement between the measurements obtained using the three different methods ($R^2 > 0.97$). The reproducibility between sample analyses was generally better than 0.1%. The TOC data are also reported on a carbonate-free basis to avoid biases related to $CaCO_3$ dilution.

4. Results

4.1. Isotope and TOC Records

At both study sites, $\delta^{13}C_{TOC}$ and $\delta^{13}C_{carb}$ values decrease in the upper part of the *tenuicostatum* zone and return to preexcursion values in the middle part of the *falciferum* zone, forming a marked and stepped 5–7‰ negative excursion defining the T-OAE (Figure 3). The high-resolution $\delta^{13}C_{TOC}$ and $\delta^{13}C_{carb}$ records at Denkingen comprise several abrupt negative shifts between 8.6 and 7 m, each with a magnitude of 1.8 to 3.8‰ (Figure 3). The initial shift toward lower $\delta^{13}C_{TOC}$ values starts 10–12 cm below that recorded by the $\delta^{13}C_{carb}$ data at both sites. The lowermost Toarcian (*tenuicostatum* zone) is notable for the occurrence of three distinct layers ("*Tafelfleins*" and "*Seegrasschiefer*"; Figure 2) [*Röhl et al*., 2001] exceeding 5% of TOC content between 9.5 m and 10.5 m. These three organic-rich layers coincide with negative excursions >3‰ in $\delta^{13}C_{TOC}$, whereas the $\delta^{13}C_{carb}$ record shows positive excursions of ~1‰ (Figure 3).

4.2. Rock-Eval Pyrolysis Data

The Rock-Eval pyrolysis measurements (Figure 3) provide a straightforward method to characterize different kerogen types and hence OM quality [*Baudin et al*., 1990; *Behar et al*., 2001]. Labile kerogen (Type II) mainly sourced from hydrogen-rich OM of algal/bacterial origin shows elevated hydrogen index (HI) values (>600 mg HC g^{-1} TOC), while low HI (<200 mg HC g^{-1} TOC) values typify hydrogen-poor kerogen of Type III (recycled/terrestrial OM). Kerogen of Type III (terrestrial/recycled OM) dominates the *spinatum* zone and most of the *tenuicostatum* zone (Figure 3) except for the three black shale horizons recording elevated HI (>300 mg HC g^{-1} TOC) and low OI (<15 mg CO_2 g^{-1} TOC). The HI shows a marked and stepped increase at the top of the *tenuicostatum* zone and remains high (>400 mg HC g^{-1} TOC) in the *falciferum* and *bifrons* zones, while the OI records its lowest values (Figure 3). These parameters indicate the predominance of marine-derived OM of Type II kerogen (see Figure S1 in the supporting information).

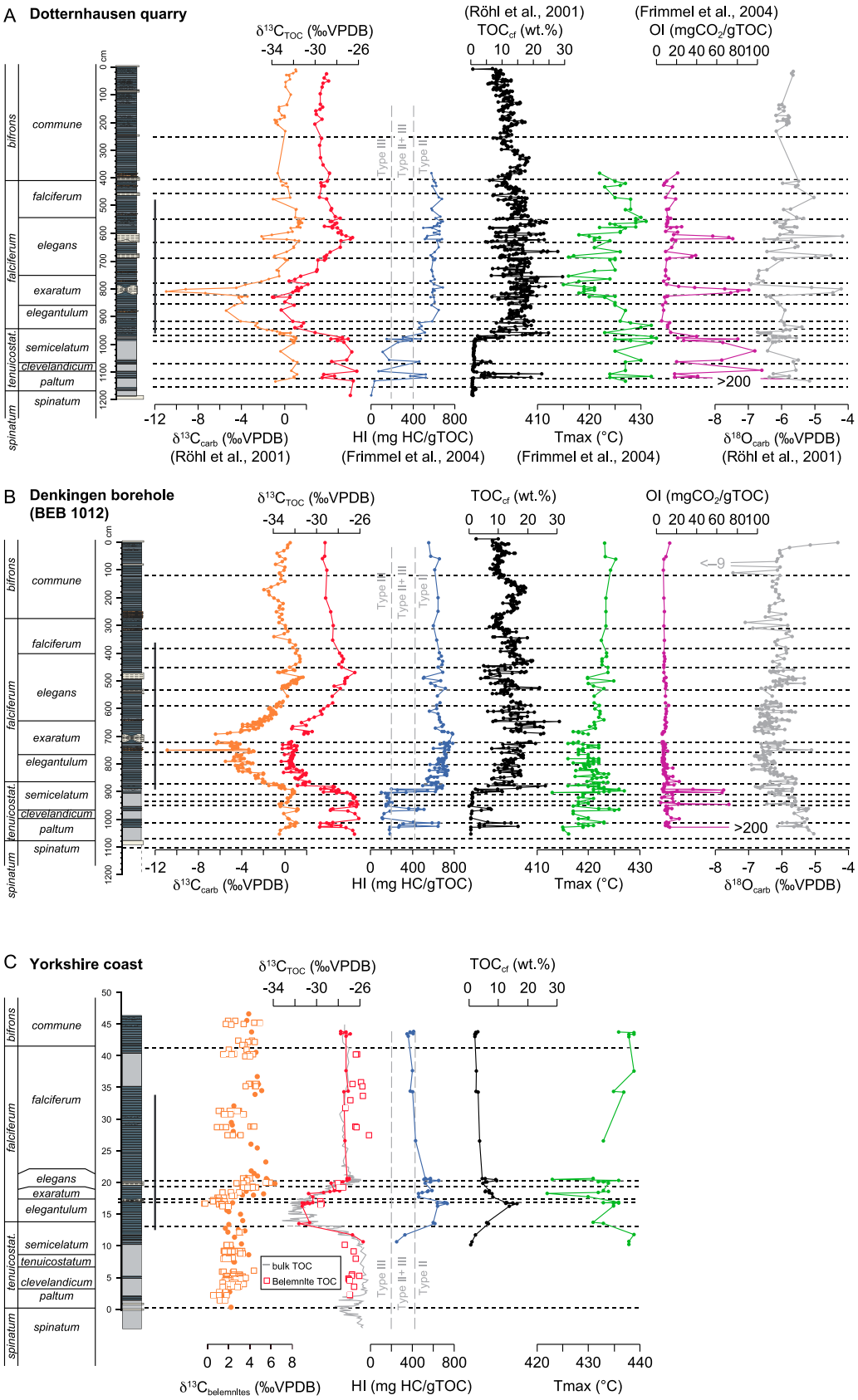
A Dotternhausen quarry
B Denkingen borehole (BEB 1012)
C Yorkshire coast
bifrons
falciferum
tenuicostat.
spinatum
commune
elegans
exaratum
elegantulum
semicelatum
clevelandicum
paltum
spinatum
tenuicostatum
δ13CTOC (‰VPDB)
TOCcf (wt.%)
(Röhl et al., 2001)
OI (mgCO2/gTOC)
(Frimmel et al., 2004)
δ13Ccarb (‰VPDB)
HI (mg HC/gTOC)
Tmax (°C)
δ18Ocarb (‰VPDB)
Type III
Type II–III
Type II
Type I
>200
<9
bulk TOC
Belemnite TOC
δ13Cbelemnites (‰VPDB)

Figure 3

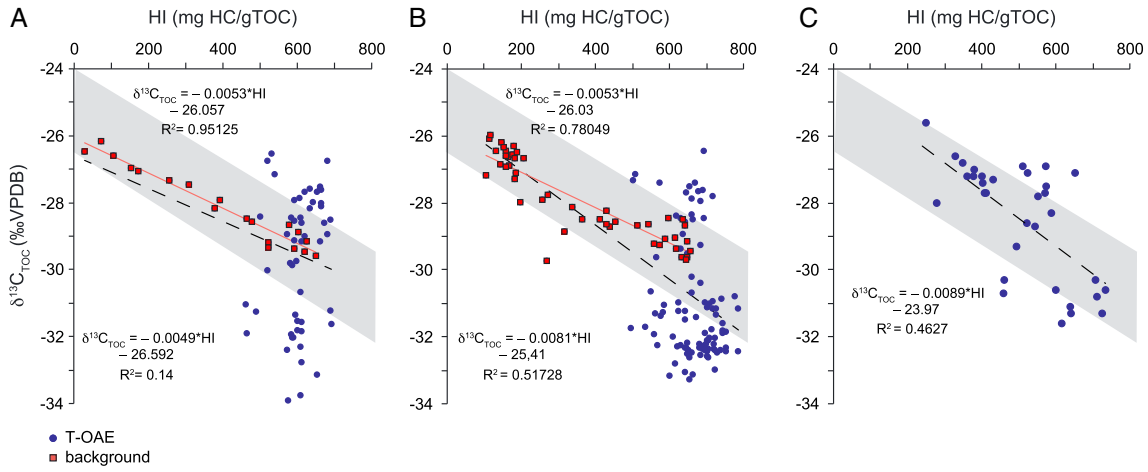

Figure 4. Relationships between $\delta^{13}C_{TOC}$ and hydrogen index. (a) Denkingen, (b), Dotternhausen, and (c) Yorkshire Coast. Least square linear regressions based on all samples (dotted lines) and on samples from outside of the T-OAE (continuous lines). See Figure 3 for the definition of the T-OAE interval in each section. The gray band shows the relationship between $\delta^{13}C_{TOC}$ and hydrogen index recorded in Jurassic and Cretaceous sediments [*Tyson*, 1995].

The T_{max} and OI values of the samples from the *tenuicostatum* zone from Dotternhausen are significantly higher than those of coeval levels from Denkingen (Figure 3). Recent weathering seems unlikely to account for these differences, as the *tenuicostatum* interval has been sampled from core material in both cases. We note that the Rock-Eval pyrolysis data from Dotternhausen [*Frimmel et al.*, 2004] were obtained on untreated samples using a Rock-Eval II *plus* device that uses a slightly different methodology for the T_{max} and OI measurements [*Behar et al.*, 2001] so that the T_{max} and OI values obtained for the two sections may not be directly comparable. The slightly higher T_{max} values recorded in the *tenuicostatum* zone at Dotternhausen (Figure 3) most likely reflect methodological differences due to the use of the Rock-Eval 2 and Rock-Eval 6 [*Behar et al.*, 2001] rather than genuine differences in thermal maturity. Similarly, these differences in the employed Rock-Eval device combined with the fact that decarbonated samples were used at Denkingen most likely account for the much higher OI values recorded in carbonate-rich beds in Dotternhausen [*Frimmel et al.*, 2004] (Figure 3). The similarity between the HI values obtained from Dotternhausen and Denkingen (Figure 3) suggests that matrix effects associated with calcium carbonate are negligible.

4.3. Source Mixing and $\delta^{13}C_{TOC}$ Ratios

In Toarcian successions of Yorkshire Coast and Argentina, the $\delta^{13}C_{TOC}$ of sediment samples dominated by Type II kerogen are 3 to 4‰ lighter than the $\delta^{13}C$ values of fossil wood collected from the same horizons [*Hesselbo et al.*, 2007; *Al-Suwaidi et al.*, 2010]. Assuming a similar 3–4‰ enrichment in ^{13}C of terrestrial OM compared to marine OM (Type II) for the entire studied time interval [*Tyson*, 1995; *Sælen et al.*, 2000; *Hesselbo et al.*, 2007], HI-$\delta^{13}C_{TOC}$ pairs are expected to plot on or close to a mixing line with a slope comprised between −0.005‰ and −0.01 (Figure 4). Our new HI and $\delta^{13}C_{TOC}$ records show an inverse relationship for the Denkingen and Dotternhausen sites with a slope (*a*) comprised between −0.005 and −0.008 that is

Figure 3. High-resolution Rock-Eval pyrolysis and geochemical records. (a) Dotternhausen, (b) Denkingen, and (c) Yorkshire Coast, UK. The dotted lines correspond to the correlation lines based on high-resolution carbonate and TOC records (see Figure 2). Kerogen types based on hydrogen index and oxygen index plots (see Figure S1 in the supporting information). The TOC and $\delta^{13}C_{carb}$ records of Dotternhausen are from *Röhl et al.* [2001]; the HI, OI, and T_{max} of Dotternhausen are from *Frimmel et al.* [2004]; the TOC, HI, T_{max}, and $\delta^{13}C_{TOC}$ records of the Yorkshire Coast are from *Sælen et al.* [2000], with additional $\delta^{13}C_{TOC}$ records (gray line) from *Cohen et al.* [2004], *Kemp et al.* [2005] and *Littler et al.* [2010]; the $\delta^{13}C_{belemnites}$ records of the Yorkshire Coast are from *Gill et al.* [2011] (circles) and *Ullmann et al.* [2014] (squares); and the $\delta^{13}C_{TOC}$ records of belemnites are from *Ullmann et al.* [2014]. Ammonite biozones and biohorizons of the Yorkshire Coast are from *Page* [2004]. The black vertical lines along the stratigraphic logs indicate the position of the T-OAE interval based on $\delta^{13}C_{carb}$ values. Abbreviations: $\delta^{13}C_{carb}$ = stable carbon isotopes of bulk carbonate; $\delta^{13}C_{TOC}$ = stable carbon isotopes of organic carbon; and TOC_{cf} = total organic carbon on a carbonate-free basis.

Table 1. Slope (a) and Intercept (b) of the HI-$\delta^{13}C_{TOC}$ Plots Obtained for the SW Germany and the Yorkshire Coast Using Different Stratigraphic Intervals[a]

Data	Interval Excluded	*a*	*b*	R^2	*n*	Amplitude $\delta^{13}C_{corr}$ CIE
		Denkingen				
All data	n/a	**−0.0081**	−25.41	0.52	143	−3.74
Outside T-OAE	355.2–887.8 cm	**−0.0053**	−26.03	0.78	46	−3.70
Outside *falciferum* zone	300.2–864.1 cm	−0.0060	−25.94	0.67	54	−3.71
		Dotternhausen				
All data	n/a	**−0.0049**	−26.59	0.14	72	−3.96
Outside T-OAE	475.5–957 cm	−0.0053	−26.05	0.95	19	−3.83
Outside *falciferum* Zone	411–937.7 cm	−0.0058	−25.97	0.88	15	−3.69
		Denkingen + Dotternhausen				
All data	n/a	**−0.0075**	−25.58	0.39	215	−3.21
Outside T-OAE	see above	−0.0053	−26.04	0.83	65	−3.76
Outside *falciferum* Zone	see above	−0.0060	−25.94	0.7	69	−3.70
		Yorkshire Coast				
All data	0	−0.0089	−23.97	0.46	33	−3.24
Outside T-OAE	13.56–34.4 m	−0.0068	−24.72	0.29	9	−3.68
Outside *falciferum* zone[b]	13.72–37.62 m	−0.0142	−22.27	0.8	9	−2.25

[a] The definition of the T-OAE interval in each section is based on the $\delta^{13}C_{carb}$ profiles shown in Figure 3. The amplitude of the CIE was calculated using the difference between maximum values before the CIE (i.e., *tenuicostatum* zone) and minimum values during the CIE (i.e., basal *falciferum* zone) based on the 5 pt moving average of the corrected $\delta^{13}C$ data.
[b] These values have not been used for the $\delta^{13}C$ correction in Figure 5 since they produce a low HI end-member (*b*) that is well below the range of **pre**excursion $\delta^{13}C$ values of fossil wood (−24 to −26‰) from the same section [*Hesselbo et al*., 2000].

compatible with a mixing line between terrestrial and marine end-members with distinct $\delta^{13}C$ signatures (Figure 4). A similar relationship is obtained for the contemporaneous strata of the Yorkshire Coast ($a = -0.0089$), which show similar albeit not identical changes in HI and $\delta^{13}C_{TOC}$ throughout the lower Toarcian interval (Figure 4).

Even stronger linear negative relationships are evident in the three sites when data of the T-OAE interval are excluded (Figure 4 and Table 1), suggesting that the link between $\delta^{13}C_{TOC}$ and OM source in this interval is complicated by superimposed changes in seawater $\delta^{13}C$. These plots imply a background $\delta^{13}C_{TOC}$ value of around −29 to −30‰ for the Type II end-member (>400 mg HC g^{-1} TOC) and a value of ~−24 to −26‰ for the more refractory kerogen of the Type III end-member (0 to 200 mg HC g^{-1} TOC). This latter end-member is in line with the $\delta^{13}C$ of fossil wood and terrestrial phytoclasts that ranges from −22 to −26‰ for most of the *tenuicostatum* zone in NW Europe (Figure 3) [*Hesselbo et al*., 2000, 2007; *Hesselbo and Pieńkowski*, 2011]. Interestingly, a similar difference in $\delta^{13}C$ between terrestrial and marine end-members (3–4‰) has been obtained for the Paleocene-Eocene Thermal Maximum (PETM) interval using a comparable mixing approach based on palynomorph assemblages [*Sluijs and Dickens*, 2012]. The calculated value of −29 to −30‰ for the Type II end-member is close to that estimated for most pre-Neogene Phanerozoic samples considered as dominated by amorphous kerogen of marine origin [*Lewan*, 1986; *Hayes et al*., 1999].

4.3.1. Correction of the $\delta^{13}C_{TOC}$ Signal

Assuming that the above $\delta^{13}C_{TOC}$-HI relationships apply for the T-OAE interval, it is now possible to calculate changes in $\delta^{13}C_{TOC}$ that are not explained by HI variations ($\delta^{13}C_{corr}$) using the following equations:

$$\delta^{13}C_{corr} = \delta^{13}C_{TOC} - \delta^{13}C_{HI} \quad (1)$$

$$\delta^{13}C_{HI} = HI*a - b \quad (2)$$

where $\delta^{13}C_{HI}$ is the $\delta^{13}C$ expected from changes in HI values and *a* and *b* are, respectively, the slope and the intercept in the HI-$\delta^{13}C_{TOC}$ plots (Figure 4). Hence, this allows us to correct the changes in $\delta^{13}C_{TOC}$ for variations in OM contribution (Figure 5). As this correction is necessarily influenced by the sample density and the arbitrary delimitation of the "perturbed" interval, different values of *a* and *b* were calculated using variable subsets of data based on various stratigraphic definitions of the T-OAE interval (Table 1). The

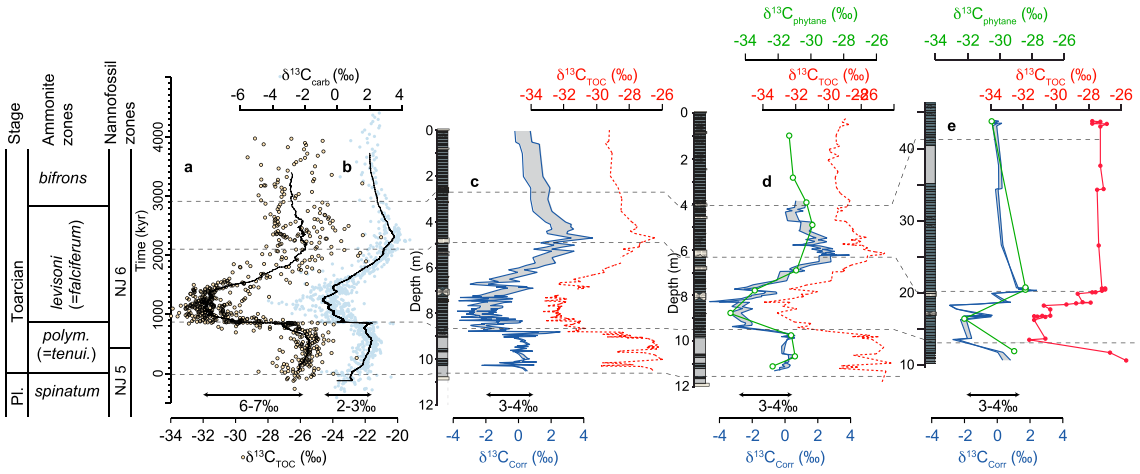

Figure 5. Comparison between the $\delta^{13}C$ profiles corrected for changing OM sourcing, bulk $\delta^{13}C_{TOC}$ profiles, and the carbon isotope composition of phytane ($\delta^{13}C_{phytane}$). (a and b) Compilation of selected $\delta^{13}C$ profiles [*Hesselbo et al.*, 2000; *Jenkyns et al.*, 2001; *Sabatino et al.*, 2009; *Kafousia et al.*, 2011; *Suan et al.*, 2011; *Hermoso et al.*, 2012] from (Figure 5a) organic carbon and (Figure 5b) carbonate isotope data plotted against the 405 kyr-tuned carbonate carbon isotope data from Peniche [*Huang and Hesselbo*, 2014], (c) Denkingen, (d) Dotternhausen, and (e) Yorkshire Coast. The $\delta^{13}C_{phytane}$ data are from *Sælen et al.* [2000] and *Schouten et al.* [2000]. The black lines represent the 21-point moving average of the compiled data. The gray envelope represents the range of values allowed by the various $\delta^{13}C_{TOC}$-HI relationships obtained by different sample categorization for each site (see Table 1). Abbreviations: Pl. = Pliensbachian; *polym.* = *polymorphum*; and *tenui.* = *tenuicostatum*.

corrected $\delta^{13}C$ profiles ($\delta^{13}C_{corr}$) are almost identical for the three sections and show relatively little dependence on the choice of the slope estimate when varying the number of samples ranked as "background" or "perturbed" (Figure 5). This correction mostly affects $\delta^{13}C$ values from the *tenuicostatum* zone, producing a long-term increase interrupted by a much reduced, ~3–4‰ negative CIE and culminating with a prominent 2‰ positive CIE in the upper part of the *falciferum* zone (Figure 5).

5. Discussion

5.1. Causes of the HI-$\delta^{13}C$ Correlation

Our interpretation of the terrestrial *versus* marine proportions of OM is substantiated by the good negative correlation between HI values and carbon preference indexes, a molecular proxy for terrestrial input based on *n*-alkanes, at Dotternhausen [*Frimmel et al.*, 2004]. The low T_{max} values recorded in the two German sections suggest limited reworking of older and thermally more mature OM (Figure 3), thus ruling out this mechanism as the main source of scatter in the HI-$\delta^{13}C_{TOC}$ plot [*Fang et al.*, 2013]. These major shifts in the OM contribution are further corroborated by palynological data from the nearby section of Zimmern [*Prauss et al.*, 1991], where prasinophyte algae and amorphous OM dominate in intervals with high HI (>400 mg HC g^{-1} TOC), while intervals with low HI preserve both terrestrial material (wood fragments, bisaccates, and spores) and oxidation-resistant material of marine origin (dinoflagellate cysts and acritarchs). Combination of high resolution, paleoecological, sedimentological, and geochemical data from Dotternhausen indicates that preservation of this Type II kerogen was strongly enhanced during prolonged anoxic intervals [*Röhl et al.*, 2001; *Frimmel et al.*, 2004; *Schwark and Frimmel*, 2004; *Röhl and Schmid-Röhl*, 2005].

Our high-resolution data show that these marked redox-driven changes in OM preservation closely track fluctuations in $\delta^{13}C_{TOC}$ not only marking the onset of the T-OAE but also those recorded in the *tenuicostatum* zone. It could be argued that $\delta^{13}C_{TOC}$ and HI are correlated because they both reflect pulses of ^{12}C- enriched carbon input that triggered greenhouse warming and increased nutrient discharge and ultimately favored anoxic conditions and the preservation of hydrogen-rich OM. This explanation requires the repeated impregnation of the ^{12}C-enriched carbon in all superficial reservoirs, a phenomenon that certainly explains the ubiquity of the T-OAE CIE and perhaps also that of the smaller negative CIE often (but not systematically) recorded by various substrates near the Pliensbachian-Toarcian boundary [*Hesselbo et al.*, 2007; *Suan et al.*, 2008a; *Littler et al.*, 2010; *Hesselbo and Pieńkowski*, 2011]. Nevertheless, this explanation

seems at odd with the positive CIEs of the $\delta^{13}C_{carb}$ recorded in the three organic-rich horizons showing the lowest $\delta^{13}C_{TOC}$ ratios in the *tenuicostatum* zone in SW Germany (Figure 3). Although the integrity of the German $\delta^{13}C_{carb}$ profiles may have been compromised by diagenesis (see section 6.2.), this explanation also fails in explaining why the marked 2–4‰ negative CIEs apparent in $\delta^{13}C_{TOC}$ records of the lower half of the *tenuicostatum* zone in SW Germany (*paltum* and *clevelandicum* subzones; Figure 3) seem systematically absent from $\delta^{13}C_{carb}$ records of coeval European sites [*Hesselbo et al*., 2007; *Sabatino et al*., 2009; *Hermoso et al*., 2012].

Another possibility is that higher atmospheric CO_2 levels, which would have also triggered anoxia and improved OM preservation indirectly, increased carbon isotopic fractionation of planktonic OM compared to inorganic reservoirs [*Hermoso et al*., 2012] and caused the recorded $\delta^{13}C_{TOC}$ troughs. A testable consequence of this hypothesis is that similar negative $\delta^{13}C_{TOC}$ troughs should occur conspicuously below the T-OAE CIE in the *tenuicostatum* zone (or in its equivalents) in other sites. Although negative $\delta^{13}C_{TOC}$ excursions have been reported in organic-rich horizons at the base of the *tenuicostatum* zone in the Yorkshire Coast [*Littler et al*., 2010], such large (2–4‰) anomalies are however absent in most other sites [*Sabatino et al*., 2009; *Hermoso et al*., 2012] and significantly, from fossil wood profiles [*Hesselbo et al*., 2007; *Hesselbo and Pieńkowski*, 2011].

In addition, we note that the post T-OAE $\delta^{13}C_{TOC}$ values (*bifrons* zone) are about 2‰ lower in SW Germany than in the Yorkshire Coast (Figure 3), a contrast hardly explainable within the context of the above hypotheses involving global processes only. We argue that such large regional differences in $\delta^{13}C_{TOC}$ can simply be accounted for by higher contribution of ^{12}C-rich Type II material in the SW German sites, in line with the higher HI values ($>600\,mg\,HC\,g^{-1}$ TOC) recorded by these two sites compared to those of the same interval ($<400\,mg\,HC\,g^{-1}$ TOC) in the Yorkshire Coast (Figure 3). This latter explanation is also advantageous in that it explains why the 3–4‰ negative $\delta^{13}C_{TOC}$ excursions of the *tenuicostatum* zone occurring between the Pliensbachian-Toarcian boundary and the T-OAE CIEs (*paltum* and *clevelandicum* subzones; Figure 3) are recorded solely in successions where organic-rich horizons are present. Repeated and global events of ^{12}C injection can hardly explain this peculiarity, unless it is assumed that erosion or nondeposition conveniently erased all the evidence for these putative global events in all documented successions except those recording organic-rich horizons.

5.2. Validity and Limitations of the Correction Procedure

The validity of the correction procedure is supported by the similarity in shape of our $\delta^{13}C_{corr}$ profiles and the $\delta^{13}C$ of phytane, a phytoplantkton-derived biomarker, in two of the sites considered here (Figure 5). In addition, the magnitude of 3–4‰ inferred from the $\delta^{13}C_{corr}$ profiles (Table 1) is similar to that recorded by $\delta^{13}C_{phytane}$ profiles in the borehole HTM 102 of the Paris Basin (3.3‰)[*van Breugel et al*., 2006] and in Yorkshire (2‰)[*French et al*., 2014], where variable mixing of terrestrial and marine OM has also been invoked to explain the larger changes recorded by the $\delta^{13}C_{TOC}$ values. Because phytane is generally thought to be primarily derived from marine photoautotrophs, these comparisons suggest that the $\delta^{13}C_{corr}$ profiles correctly approximate changes in the $\delta^{13}C$ of marine OM in the studied areas. We note, however, that the resolution of available $\delta^{13}C_{phytane}$ profiles is low (Figure 3), so that further high-resolution compound-specific $\delta^{13}C$ records are needed to confirm or infirm the validity of our corrected profile at a finer scale.

By contrast, the magnitude of the CIE in fossil wood [*Hesselbo et al*., 2007; *Hesselbo and Pieńkowski*, 2011] is about twice as large (7–10‰) as that recorded by bulk carbonate and kerogen of Type II (3–4‰; Figure 5). Although changes in wood-producing taxa [*Schouten et al*., 2007] may explain these differences in amplitude, it is likely that the carbon-isotope fractionation of C3 plants relative to ambient CO_2 increased during the T-OAE, perhaps due to increased atmospheric CO_2 levels or water availability [*Hesselbo et al*., 2007; *Hesselbo and Pieńkowski*, 2011]. This latter mechanism appears particularly attractive since modern C3 plants show a strong dependency on mean annual precipitation regimes [*Kohn*, 2010]. Besides, evidence for considerable changes in pCO_2 exist for the T-OAE interval [*McElwain et al*., 2005].

These various lines of evidence imply that the difference between Type II and III kerogen most assuredly did not remain constant across the T-OAE, and thus compromise the reconstruction of the $\delta^{13}C$ of terrestrial OM

based on Type II-dominated sections, such as those studied here in Germany. Therefore, the $\delta^{13}C_{corr}$ profiles presented herein should be considered as a first-order approximation of the $\delta^{13}C$ of the Type II material and cannot be used to infer the $\delta^{13}C$ of terrestrial reservoirs. In addition, we note that today's C3 plants show large latitudinal $\delta^{13}C$ gradients [*Freeman*, 2001; *Kohn*, 2010], whereas the offset between marine and terrestrial OM has changed substantially over long time periods, with the marine OM being lighter or heavier than terrestrial OM depending on the time interval [*Hayes et al*., 1999; *Sælen et al*., 2000; *Sluijs and Dickens*, 2012]. Accordingly, the slope and direction of the HI-$\delta^{13}C_{TOC}$ is expected to vary significantly as a function of the paleolatitude and age of the considered deposits and should therefore not be extrapolated spatially and temporally without careful appraisal. Moreover, some commonly encountered minerals such as calcium carbonate and clay minerals may artificially decrease HI values of Type II kerogen [*Espitalié et al*., 1984; *Spiro*, 1991]. Such biases are also expected to vary spatially and should thus also be taken into consideration before comparing the slope and intercept of the HI-$\delta^{13}C_{TOC}$ relationships from different sites. For instance, such matrix effects may account for the difference in the slope value obtained between the Yorkshire Coast and SW German sites (Figure 4). Matrix effect due to different calcium carbonate content is ruled out by the similarity of HI values obtained in the two German sites (see section 4.2) and by the fact that decarbonated samples were also used in the study of *Sælen et al*. [2000]. Similarly, the almost identical intercept and slope of the TOC *versus* S_2 peak plots of the samples from Denkingen and Yorkshire Coast suggest similar retention effects at low TOC [*Langford and Blanc-Valleron*, 1990] in both regions (see Figure S2 in the supporting information). However, laboratory experiments show that even at high TOC contents (>4 wt.%), HI values may vary as much as 200 mg HC g^{-1} TOC when different clay minerals are admixed with the same kerogen [*Spiro*, 1991]. Further HI and $\delta^{13}C_{TOC}$ measurements on separated kerogen are thus required to determine whether the different HI-$\delta^{13}C_{TOC}$ slopes obtained in Yorkshire and Germany reflect matrix effects, contrasting paleoenvironmental conditions or sampling biases.

Another requirement of the correction procedure is that a sufficiently high number of samples outside the "perturbed" interval are taken into account so that the background trends between HI and $\delta^{13}C_{TOC}$ can be appropriately defined. The HI-$\delta^{13}C_{TOC}$ relationship in the T-OAE interval being complicated by large changes in seawater $\delta^{13}C$, a sampling focusing mostly on this interval at Denkingen, would for instance reveal almost no correlation between HI and $\delta^{13}C_{TOC}$, which would lead to the misleading conclusion that the record is entirely primary. Despite these limitations, the use of HI values is advantageous in that it allows the characterization of the same bulk organic material as that analyzed for $\delta^{13}C_{TOC}$, by contrast to biomarker or palynomorph assemblages [*Sluijs and Dickens*, 2012], which generally represent only a small fraction of the bulk organic carbon. In this regard, the comparison of HI and $\delta^{13}C_{TOC}$ data provides a rapid and cost-effective method, which should be considered complementary to the $\delta^{13}C$ characterization of individual molecular compounds [*Schouten et al*., 2000; *French et al*., 2014] or isolated palynomorph fractions [*Sluijs et al*., 2007] in the $\delta^{13}C$-based studies of past carbon cycle perturbations.

6. Implications for Chemostratigraphic Correlations and Carbon Cycling

6.1. Influence of Productivity and Oxygenation on $\delta^{13}C_{TOC}$ Records

Because the type of OM preserved in the sediment is largely controlled by bottom water oxygenation and climate, our findings imply that the amplitude and shape of the CIE recorded by $\delta^{13}C_{TOC}$ across the T-OAE should have a strong dependence on the paleogeographic gradients in productivity and oxygenation. This assumption is supported by the anomalously low $\delta^{13}C_{TOC}$ values (−29 to −27‰) recorded after the T-OAE in Germany, Yorkshire, E France, and N Siberia [*Cohen et al*., 2004; *van Breugel et al*., 2006; *Suan et al*., 2011], where black shales and evidence for anoxia are found up to the *bifrons* ammonite zone [*Röhl et al*., 2001; *van Breugel et al*., 2006; *Suan et al*., 2011], which can be accounted for by improved preservation of ^{12}C-enriched marine OM under oxygen-depleted conditions. Conversely, preferential preservation of more refractory, ^{13}C-enriched terrestrial OM under well-oxygenated conditions explains the substantially higher $\delta^{13}C_{TOC}$ values (−25 to −22‰) recorded after the T-OAE in several Tethyan sites [*Sabatino et al*., 2009; *Kafousia et al*., 2011]. Our correction also removes the first two shifts in $\delta^{13}C_{TOC}$ in the uppermost *tenuicostatum* zone, previously interpreted as evidence for global pulses of ^{12}C injection [*Kemp et al*., 2005; *Cohen et al*., 2007; *Hesselbo and Pieńkowski*, 2011] and helps to explain the lag between the shifts in $\delta^{13}C_{carb}$ and $\delta^{13}C_{TOC}$ (Figures 3 and 5).

These data strongly suggest that improved marine OM preservation under oxygen-depleted conditions has the ability to produce "artificial" $\delta^{13}C_{TOC}$ excursions, i.e., anomalies that do not necessarily reflect local or global changes in the $\delta^{13}C$ of the dissolved inorganic carbon (DIC) pools. As mentioned above, in many NW European sites, the interval recording the negative CIE of the lower part of the *falciferum* zone is followed by thick black shale deposits characterized by low $\delta^{13}C_{TOC}$ [*Prauss et al*., 1991; *van Breugel et al*., 2006]. The resulting "double" negative CIE, in the absence of high-resolution biostratigraphic control, could be misleadingly interpreted as representing the T-OAE interval. Such a prolonged episode of improved preservation of ^{12}C-rich OM would for instance explain why the tuffs found in an expanded (>30 m) succession of Toarcian black shale in Argentina yield anomalously young ages and an overly long duration for the double CIE attributed to the T-OAE [*Mazzini et al*., 2010].

6.2. Variability of the Carbon Isotope Profiles Among Various Substrates

Our findings help to address the long-standing debate concerning the causes of the marked contrast between the 6–7‰ CIE evident from most $\delta^{13}C_{TOC}$ profiles and more subdued 2‰ CIE recorded by belemnites from Dotternhausen [*van de Schootbrugge et al*., 2005; *Gill et al*., 2011]. The 3–4‰ negative CIE of the $\delta^{13}C_{corr}$ profile (Table 1) reduces significantly the difference between both profiles and hence the amount of isotopic change that has to be attributed to ecological [*Hesselbo et al*., 2007; *Ullmann et al*., 2014] or paleoceanographic [*van de Schootbrugge et al*., 2005] biases in order to reconcile both records.

Most inorganic ($\delta^{13}C_{carb}$) records of the T-OAE show a broad 3–4‰ positive excursion interrupted by a 2–3‰ negative CIE, while $\delta^{13}C_{TOC}$ record a negative trend starting with a 6–7‰ CIE (Figure 5). Notable exceptions to these patterns are the $\delta^{13}C_{carb}$ profiles from SW Germany, which show significantly lower values and have a much larger magnitude than that from most other European sections (Figures 3 and 5). Although this geographic variability may reflect differences in the local water mass geochemistry, several lines of evidence suggest that the $\delta^{13}C_{carb}$ records showing the largest magnitude are also affected by stratigraphic changes in composition of the carbonate particles carrying the isotope signals. The large magnitude in SW Germany is indeed most likely exaggerated by the increased contribution of authigenic carbonate formed from the ^{12}C-enriched carbon derived from OM degradation by sulfate-reducing bacteria during the T-OAE [*Röhl et al*., 2001]. The prevalence of this process in the study sites is indeed illustrated by the extremely low $\delta^{13}C_{carb}$ values of the numerous concretionary beds of clear diagenetic origin occurring in the succession [*Röhl et al*., 2001] and the presence of abundant authigenic inframicrometric crystallites in the fine fraction [*Bour et al*., 2007]. Substantial modification of the carbonate sediment chemistry of the studied sites is additionally suggested by the discontinuous occurrence of sparitic moulds of small gastropod shells (*Coelodiscus*) within shale beds [*Riegraf et al*., 1984]. As observed in similar successions in S France [*Riegraf et al*., 1984; *Suan et al*., 2013], these shells occur abundantly in authigenic concretions, whereas they are totally absent in coeval shale laminae [*Riegraf et al*., 1984], suggesting that extensive dissolution-recrystallization processes occurred within these levels during early diagenesis. Such processes are further exemplified by the $\delta^{18}O_{carb}$ values at both study sites, which are comprised between −4 and −7‰ in both sections, with the lowest and highest values being generally recorded in the carbonate-poor and carbonate-rich lithologies, respectively (Figure 3). As noted previously for Dotternhausen [*Röhl et al*., 2001], these relationships, combined to extremely low values recorded throughout both sections, imply a strong diagenetic control of the $\delta^{18}O_{carb}$ and $\delta^{13}C_{carb}$ records. Higher authigenic inframicrometric crystallite contribution might also be invoked as a possible cause of the large magnitude (6‰) of the $\delta^{13}C_{carb}$ negative CIE at Sancerre [*Hermoso et al*., 2009]. The $\delta^{13}C_{carb}$ values of monocrystalline particles in the samples recording the lowest portion of the CIE at this site are indeed 1.5‰ lighter than other isolated microfractions, which also contain higher proportions of authigenic monocrystals in this interval [*Hermoso et al*., 2009]. If the sample with the highest authigenic microcrystalline content is excluded from the isolated microfraction curve of *Hermoso et al*. [2009], the magnitude of the CIE is reduced from 4.4‰ to 3.5‰, i.e., fully comparable with the magnitude (3–4‰) evident from our corrected curves (Figure 6).

Apart from these examples, the amplitude and shape of the CIE of the $\delta^{13}C_{corr}$ are very similar to most coeval carbonate records (Figure 5) and particularly that of brachiopods from Portugal [*Suan et al*., 2010], which constitutes one of the rare isotopic records from nonmotile animals for this interval.

Experimental studies suggest that both the $\delta^{13}C$ and $\delta^{18}O$ composition of planktic foraminifera increase with decreasing seawater [CO_3^{2-}] and pH [*Spero et al*., 1997]. It could be argued, therefore, that the magnitude of the T-OAE $\delta^{13}C$ records obtained from carbonate material was dampened by a major decrease in pH, similar to that proposed for records of the PETM [*Uchikawa and Zeebe*, 2010]. The underestimation of the magnitude of the PETM CIE due to pH decline may have reached 2.1‰ in deep-sea sediments, where the most severe decrease in pH occurred, but probably did not exceed 0.5–1‰ in superficial water (0–100 m) [*Uchikawa and Zeebe*, 2010]. Assuming a similar response of ocean pH to massive carbon injection during the T-OAE, it thus appears unlikely that pH-induced changes in fractionation would have exceeded 1‰ in relatively shallow water settings characterizing all known $\delta^{13}C_{carb}$ records of the T-OAE. Accordingly, the 2 to 3‰ shift to lower $\delta^{13}C$ values recorded by bulk carbonate at the onset of the T-OAE (Figure 5) may be a slight underestimation of $\delta^{13}C$ changes that affected the superficial marine DIC. An inferred magnitude of 3–4‰ is not only compatible with the $\delta^{13}C_{corr}$ and $\delta^{13}C_{phytane}$ profiles but also with the $\delta^{13}C$ of OM extracted from belemnites (Figures 3 and 5). These changes in the belemnite $\delta^{13}C$ of OM likely reflects changes in $\delta^{13}C$ of the organic carbon of belemnite preys and should be unaffected by pH effects [*Ullmann et al*., 2014]. We therefore suggest that taking into account the varying contribution of terrestrial and marine OM with different $\delta^{13}C$ signatures helps to reconcile most $\delta^{13}C$ records of the T-OAE.

The similarity between our $\delta^{13}C_{corr}$ profiles and most $\delta^{13}C_{carb}$ records suggests relatively constant fractionation between Type II (bacterial/algal) material and superficial DIC during the T-OAE in the western margin of the Tethys Ocean. This finding might appear surprising given the fact that atmospheric CO_2 increased across the T-OAE [*McElwain et al*., 2005], a condition that should have increased carbon isotope fractionation (ε_p) of phytoplanktonic OM [*Popp et al*., 1998]. Nevertheless, the phytoplanktonic species showing the highest changes in ε_p as a response to high pCO_2 levels were either rare (coccolithoporids) or absent (diatoms) in Early Jurassic oceans. In some ubiquitous marine cyanobacteria such as *Synechococcus*, the ε_p shows no relationship with CO_2 concentrations [*Popp et al*., 1998]. If such relation holds true for all cyanobacteria, elevated contribution to the Type II kerogen by cyanobacteria might therefore explain the limited difference between the $\delta^{13}C_{corr}$ and $\delta^{13}C_{carb}$ profiles. Such contribution is compatible with the very low nitrogen isotope values recorded in strata spanning the T-OAE, which have been interpreted as evidence for massive cyanobacteria blooms recorded before, during, and after the T-OAE [*Sælen et al*., 2000; *Jenkyns et al*., 2001]. In any case, these results seriously compromise the use of difference between $\delta^{13}C_{TOC}$ and $\delta^{13}C_{carb}$ in marine strata as a reliable pCO_2 proxy across the T-OAE.

6.3. Implications for the Cause of the T-OAE Carbon Cycle Perturbations

Collectively, our data indicate that changes in $\delta^{13}C$ of the superficial DIC in the western Tethys at the onset of the T-OAE did most likely not exceed 3 to 4‰, i.e., much less than previously appreciated from TOC records alone [*Kemp et al*., 2005; *Cohen et al*., 2007]. Since the results of carbon cycle modeling rely heavily on the magnitude of carbon isotope changes [*Beerling and Brentnall*, 2007], our data provide essential constraints for future simulations of the potential driving mechanisms of Toarcian carbon cycle perturbations. Numerical simulations suggest that the release of ~6000–9000 Gt C of clathrate CH_4 ($\delta^{13}C = -60‰$) or ~15,000–25,000 Gt of thermogenic CH_4 ($\delta^{13}C = -40‰$) can produce a CIE of this magnitude [*Beerling and Brentnall*, 2007] but only increase mean global temperatures by 2–3°C, i.e., much less than the >7°C warming suggested by T-OAE oxygen isotope records [*Bailey et al*., 2003; *Suan et al*., 2010]. Unless this warming and the CIE were forced by distinct carbon sources, our $\delta^{13}C_{corr}$ profiles thus imply the release of much larger amounts of carbon with a much more ^{13}C-enriched signature than previously modeled. Furthermore, our results reveal a long-term rise in $\delta^{13}C$ across the T-OAE that was initially only evident from $\delta^{13}C_{carb}$ data and attributed to globally enhanced rates of organic carbon burial [*Jenkyns*, 1988]. When combined to the positive limb of the negative CIE, this shift exceeds 4‰ in all substrates and indeed corresponds to one of the most dramatic carbon isotope features known in Mesozoic strata. This positive $\delta^{13}C$ shift, although considered as a key feature in early geochemical studies of the T-OAE [*Jenkyns*, 1988; *Jenkyns and Clayton*, 1997], has up till now attracted much less attention than its negative precursor. This $\delta^{13}C$ shift suggests the burial of huge amounts of organic carbon within a few hundred thousands of years and certainly deserves further modeling efforts.

7. Conclusions

The CIE in $\delta^{13}C_{TOC}$ records of the T-OAE is considerably exaggerated by varying proportions of terrestrial and marine organic matter. The $\delta^{13}C$ data corrected for changing OM sourcing indicate no change in carbon isotope fractionation between organic and inorganic pools across the T-OAE, a result that may point to a major role of cyanobacteria as OM producers during the Early Jurassic. Furthermore, the corrected 3–4‰ CIE, if representative of the whole oceanic reservoir, implies the injection of larger amounts of carbon than previously modeled. Beyond the T-OAE debate, the negative correlation between HI and $\delta^{13}C_{TOC}$ evident from the studied sections is similar to that recorded by most pre-Neogene marine sedimentary rocks [*Dean et al*., 1986; *Tyson*, 1995], suggesting a long-lived link between OM source and $\delta^{13}C_{TOC}$. Taking into account the age and paleolatitude of the considered samples, the simple procedure presented herein might thus be particularly advantageous for improving carbon cycle reconstructions for other intervals characterized by coeval changes in $\delta^{13}C_{TOC}$ and OM quality, such as those recorded in marine sediments deposited during Cretaceous OAEs, the end-Permian, and end-Triassic events [*van de Schootbrugge et al*., 2008; *Hays et al*., 2012].

Acknowledgments

G. Suan gratefully acknowledges postdoctoral support from the Alexander von Humboldt Foundation. We are grateful to S. Hofmann (Goethe Frankfurt University) for the help with carbon isotope analyses. We thank A. Schmid-Röhl for sharing with us the TOC and $CaCO_3$ data from SW Germany, D.R. Gröcke, G.R. Dickens, P. Wignall, F. Baudin, and an anonymous reviewer for their constructive remarks on earlier versions of the manuscript. The data used to produce the results of this paper are available in the supporting information.

References

Al-Suwaidi, A. H., G. N. Angelozzi, F. Baudin, S. E. Damborenea, S. P. Hesselbo, H. C. Jenkyns, M. O. Mancenido, and A. C. Riccardi (2010), First record of the Early Toarcian oceanic anoxic event from the Southern Hemisphere, Neuquen Basin, Argentina, *J. Geol. Soc.*, *167*(4), 633–636.

Bailey, T. R., Y. Rosenthal, J. M. McArthur, B. van de Schootbrugge, and M. F. Thirlwall (2003), Paleoceanographic changes of the Late Pliensbachian-Early Toarcian interval: A possible link to the genesis of an oceanic anoxic event, *Earth Planet. Sci. Lett.*, *212*, 307–320.

Baudin, F., J. P. Herbin, and M. Vandenbroucke (1990), Mapping and geochemical characterization of the Toarcian organic matter in the Mediterranean Tethys and Middle East, *Org. Geochem.*, *16*(4–6), 677–687.

Beerling, D. J., and S. J. Brentnall (2007), Numerical evaluation of mechanisms driving Early Jurassic changes in global carbon cycling, *Geology*, *35*(3), 247–250.

Behar, F., V. Beaumont, and H. L. D. B. Penteado (2001), Technologie Rock-Eval 6: Performances et développements, *Oil Gas Sci. Technol.- Rev. IFP*, *56*(2), 111–134.

Boulila, S., B. Galbrun, E. Huret, L. A. Hinnov, I. Rouget, S. Gardin, and A. Bartolini (2014), Astronomical calibration of the Toarcian Stage: Implications for sequence stratigraphy and duration of the early Toarcian OAE, *Earth Planet. Sci. Lett.*, *386*, 98–111.

Bour, I., E. Mattioli, and B. Pittet (2007), Nannofacies analysis as a tool to reconstruct paleoenvironmental changes during the Early Toarcian anoxic event, *Palaeogeogr. Palaeoclimatol. Palaeoecol.*, *249*(1–2), 58–79.

Brazier, J.-M., G. Suan, T. Tacail, L. Simon, J. E. Martin, E. Mattioli, and V. Balter (2015), Calcium isotope evidence for dramatic increase of continental weathering during the Toarcian oceanic anoxic event (Early Jurassic), *Earth Planet. Sci. Lett.*, *411*, 164–176.

Cohen, A. S., A. L. Coe, S. M. Harding, and L. Schwark (2004), Osmium isotope evidence for the regulation of atmospheric CO_2 by continental weathering, *Geology*, *32*(2), 157–160.

Cohen, A. S., A. L. Coe, and D. B. Kemp (2007), The late Paleocene-Early Eocene and Toarcian (Early Jurassic) carbon isotope excursions: A comparison of their time scales, associated environmental changes, causes and consequences, *J. Geol. Soc.*, *164*, 1093–1108.

Dean, W. E., M. A. Arthur, and G. E. Claypool (1986), Depletion of ^{13}C in Cretaceous marine organic matter: Source, diagenetic, or environmental sigal?, *Mar. Geol.*, *70*(1–2), 119–157.

Espitalié, J., K. Senga Makadi, and J. Trichet (1984), Role of the mineral matrix during kerogen pyrolysis, *Org. Geochem.*, *6*, 365–382.

Fang, L., C. J. Bjerrum, S. P. Hesselbo, U. Kotthoff, F. M. G. McCarthy, B. Huang, and P. W. Ditchfield (2013), Carbon-isotope stratigraphy from terrestrial organic matter through the Monterey event, Miocene, New Jersey margin (IODP Expedition 313), *Geosphere*, *9*(5), 1303–1318.

Freeman, K. H. (2001), Isotopic biogeochemistry of marine organic carbon, *Rev. Mineral. Geochem.*, *43*(1), 579–605.

Freeman, K. H., and J. M. Hayes (1992), Fractionation of carbon isotopes by phytoplankton and estimates of ancient CO_2 levels, *Global Biogeochem. Cycles*, *6*(2), 185–198, doi:10.1029/92GB00190.

French, K. L., J. Sepúlveda, J. Trabucho-Alexandre, D. R. Gröcke, and R. E. Summons (2014), Organic geochemistry of the early Toarcian oceanic anoxic event in Hawsker Bottoms, Yorkshire, England, *Earth Planet. Sci. Lett.*, *390*, 116–127.

Frimmel, A. (2003), Hochauflösende Untersuchungen von Biomarkern an epikontinentalen Schwarzschiefern des Unteren Toarciums (Posidonienschiefer, Lias ε) von SW-Deutschland Unpublished PhD thesis, p. 121, Universität Tübingen, Tübingen.

Frimmel, A., W. Oschmann, and L. Schwark (2004), Chemostratigraphy of the posidonia Black Shale, SW Germany I. Influence of sea level variation on organic facies evolution, *Chem. Geol.*, *206*(3–4), 199–230.

Gill, B. C., T. W. Lyons, and H. C. Jenkyns (2011), A global perturbation to the sulfur cycle during the Toarcian oceanic anoxic event, *Earth Planet. Sci. Lett.*, *312*(3–4), 484–496.

Hayes, J. M., H. Strauss, and A. J. Kaufman (1999), The abundance of ^{13}C in marine organic matter and isotopic fractionation in the global biogeochemical cycle of carbon during the past 800 Ma, *Chem. Geol.*, *161*(1–3), 103–125.

Hays, L. E., K. Grice, C. B. Foster, and R. E. Summons (2012), Biomarker and isotopic trends in a Permian-Triassic sedimentary section at Kap Stosch, Greenland, *Org. Geochem.*, *43*, 67–82.

Hermoso, M., L. Le Callonnec, F. Minoletti, M. Renard, and S. P. Hesselbo (2009), Expression of the Early Toarcian negative carbon-isotope excursion in separated carbonate microfractions (Jurassic, Paris Basin), *Earth Planet. Sci. Lett.*, *277*(1–2), 194–203.

Hermoso, M., F. Minoletti, R. E. M. Rickaby, S. P. Hesselbo, F. Baudin, and H. C. Jenkyns (2012), Dynamics of a stepped carbon-isotope excursion: Ultra high-resolution study of Early Toarcian environmental change, *Earth Planet. Sci. Lett.*, *319-320*, 45–54.

Hermoso, M., F. Minoletti, and P. Pellenard (2013), Black shale deposition during Toarcian super-greenhouse driven by sea level, *Clim. Past*, *9*(6), 2703–2712.

Hesselbo, S. P., and G. Pieńkowski (2011), Stepwise atmospheric carbon-isotope excursion during the Toarcian oceanic anoxic event (Early Jurassic, Polish Basin), *Earth Planet. Sci. Lett.*, *301*(1–2), 365–372.

Hesselbo, S. P., D. R. Grocke, H. C. Jenkyns, C. J. Bjerrum, P. Farrimond, H. S. M. Bell, and O. R. Green (2000), Massive dissociation of gas hydrate during a Jurassic oceanic anoxic event, *Nature*, *406*(6794), 392–395.

Hesselbo, S. P., H. C. Jenkyns, L. V. Duarte, and L. C. V. Oliveira (2007), Carbon-isotope record of the Early Jurassic (Toarcian) oceanic anoxic event from fossil wood and marine carbonate (Lusitanian Basin, Portugal), *Earth Planet. Sci. Lett.*, *253*(3–4), 455–470.

Huang, C., and S. P. Hesselbo (2014), Pacing of the Toarcian oceanic anoxic event (Early Jurassic) from astronomical correlation of marine sections, *Gondwana Res.*, *25*(4), 1348–1356.

Jenkyns, H. C. (1988), The Early Toarcian (Jurassic) Anoxic Event - stratigraphic, sedimentary, and geochemical evidence, *Am. J. Sci.*, *288*(2), 101–151.

Jenkyns, H. C. (2010), Geochemistry of oceanic anoxic events, *Geochem., Geophys., Geosyst.*, *11*, Q03004, doi:10.1029/2009GC002788.

Jenkyns, H. C., and C. J. Clayton (1997), Lower Jurassic epicontinental carbonates and mudstones from England and Wales: Chemostratigraphic signals and the early Toarcian anoxic event, *Sedimentology*, *44*(4), 687–706.

Jenkyns, H. C., D. R. Grocke, and S. P. Hesselbo (2001), Nitrogen isotope evidence for water mass denitrification during the early Toarcian (Jurassic) oceanic anoxic event, *Paleoceanography*, *16*(6), 593–603, doi:10.1029/2000PA000558.

Kafousia, N., V. Karakitsios, H. C. Jenkyns, and E. Mattioli (2011), A global event with a regional character: The Early Toarcian oceanic anoxic event in the Pindos Ocean (northern Peloponnese, Greece), *Geol. Mag.*, *148*(4), 619–631.

Kemp, D. B., and K. Izumi (2014), Multiproxy geochemical analysis of a Panthalassic margin record of the early Toarcian oceanic anoxic event (Toyora area, Japan), *Palaeogeogr. Palaeoclimatol. Palaeoecol.*, *414*, 332–341.

Kemp, D. B., A. L. Coe, A. S. Cohen, and L. Schwark (2005), Astronomical pacing of methane release in the Early Jurassic period, *Nature*, *437*(7057), 396–399.

Kohn, M. J. (2010), Carbon isotope compositions of terrestrial C3 plants as indicators of (paleo)ecology and (paleo)climate, *Proc. Natl. Acad. Sci. U. S. A.*, *107*(46), 19,691–19,695.

Küspert, W. (1982), Environmental changes during oil shale deposition as deduced from stable isotope ratios, in *Cyclic and Event Stratification*, edited by G. Einsele and A. Seilacher, pp. 482–501, Springer, Berlin.

Langford, F. F., and M.-M. Blanc-Valleron (1990), Interpreting Rock-Eval Pyrolysis data using graphs of pyrolizable hydrocarbons versus total organic carbon, *Am. Assoc. Petrol. Geol. Bull.*, *74*(6), 799–804.

Lewan, M. D. (1986), Stable carbon isotopes of amorphous kerogens from Phanerozoic sedimentary rocks, *Geochim. Cosmochim. Acta*, *50*(8), 1583–1591.

Littler, K., S. P. Hesselbo, and H. C. Jenkyns (2010), A carbon-isotope perturbation at the Pliensbachian-Toarcian boundary: Evidence from the Lias Group, NE England, *Geol. Mag.*, *147*(2), 181–192.

Mattioli, E., B. Pittet, G. Suan, and S. Mailliot (2008), Calcareous nannoplankton changes across the early Toarcian oceanic anoxic event in the Western Tethys, *Paleoceanography*, *23*, PA3208, doi:10.1029/2007PA001435.

Mattioli, E., B. Pittet, L. Petitpierre, and S. Mailliot (2009), Dramatic decrease of pelagic carbonate production by nannoplankton across the Early Toarcian anoxic event (T-OAE), *Global Planet. Change*, *65*(3–4), 134–145.

Mazzini, A., H. Svensen, H. A. Leanza, F. Corfu, and S. Planke (2010), Early Jurassic shale chemostratigraphy and U-Pb ages from the Neuquen Basin (Argentina): Implications for the Toarcian oceanic anoxic event, *Earth Planet. Sci. Lett.*, *297*(3–4), 633–645.

McElwain, J. C., J. Wade-Murphy, and S. P. Hesselbo (2005), Changes in carbon dioxide during an oceanic anoxic event linked to intrusion into Gondwana coals, *Nature*, *435*, 479–482.

Page, K. N. (2004), A sequence of biohorizons for the subboreal province Lower Toarcian in Northern Britain and their correlation with a submediterranean standard, *Riv. Ital. Paleontol. Stratigr.*, *110*(1), 109–114.

Popp, B. N., E. A. Laws, R. R. Bidigare, J. E. Dore, K. L. Hanson, and S. G. Wakeham (1998), Effect of phytoplankton cell geometry on carbon isotopic fractionation, *Geochim. Cosmochim. Acta*, *62*(1), 69–77.

Prauss, M., B. Ligouis, and H. Luterbacher (1991), Organic matter and palynomorphs in the 'Posidonienschiefer' (Toarcian, Lower Jurassic) of southern Germany, *Geol. Soc. London Spec. Publ.*, *58*(1), 335–351.

Riegraf, W., G. Werner, and F. Lörcher (1984), *Der Posidonienschiefer: Biostratigraphie, Fauna und Fazies des südwestdeutschen Untertoarciums (Lias Epsilon)*, pp. 195 , Ferdinand Enke Verlag, Stuttgart.

Röhl, H. J., and A. Schmid-Röhl (2005), Lower Toarcian (Upper Liassic) black shales of the Central European Epicontinental basin: A sequence stratigraphic case study from the SW German Posidonia Shale, in *Deposition of Organic-Carbon-Rich Sediments: Models, Mechanisms, and Consequences*, pp. 165–189, SEPM Spec. Publ., 82.

Röhl, H.-J., A. Schmid-Röhl, W. Oschmann, A. Frimmel, and L. Schwark (2001), The Posidonia shale (Lower Toarcian) of SW-Germany: An oxygen-depleted ecosystem controlled by sea level and paleoclimate, *Palaeogeogr. Palaeoclimatol. Palaeoecol.*, *169*, 273–299.

Sabatino, N., R. Neri, A. Bellanca, H. C. Jenkyns, F. Baudin, G. Parisi, and D. Masetti (2009), Carbon-isotope records of the Early Jurassic (Toarcian) oceanic anoxic event from the Valdorbia (Umbria-Marche Apennines) and Monte Mangart (Julian Alps) sections: Paleoceanographic and stratigraphic implications, *Sedimentology*, *56*(5), 1307–1328.

Sælen, G., R. V. Tyson, N. Telnæs, and M. R. Talbot (2000), Contrasting water mass conditions during deposition of the Whitby Mudstone (Lower Jurassic) and Kimmeridge Clay (Upper Jurassic) formations, UK, *Palaeogeogr. Palaeoclimatol. Palaeoecol.*, *163*(3–4), 163–196.

Schmid-Röhl, A. (1999), Hochauflösende geochemische Untersuchungen im Posidonienschiefer (Lias ε) von SW-Deutschland, *Tübinger Geowiss. Arb. A*, *48*, 1–189.

Schouten, S., H. M. E. van Kaam-Peters, W. I. C. Rijpstra, M. Schoell, and J. S. Sinninghe Damste (2000), Effects of an oceanic anoxic event on the stable carbon isotopic composition of early Toarcian carbon, *Am. J. Sci.*, *300*(1), 1–22.

Schouten, S., M. Woltering, W. I. C. Rijpstra, A. Sluijs, H. Brinkhuis, and J. S. S. Damste (2007), The Paleocene-Eocene carbon isotope excursion in higher plant organic matter: Differential fractionation of angiosperms and conifers in the Arctic, *Earth Planet. Sci. Lett.*, *258*(3–4), 581–592.

Schwark, L., and A. Frimmel (2004), Chemostratigraphy of the Posidonia Black Shale, SW-Germany II. Assessment of extent and persistence of photic-zone anoxia using aryl isoprenoid distributions, *Chem. Geol.*, *206*(3–4), 231–248.

Sluijs, A., and G. R. Dickens (2012), Assessing offsets between the δ13C of sedimentary components and the global exogenic carbon pool across early Paleogene carbon cycle perturbations, *Global Biogeochem. Cycles*, *26*, GB4005, doi:10.1029/2011GB004224.

Sluijs, A., H. Brinkhuis, S. Schouten, S. M. Bohaty, C. M. John, J. C. Zachos, G. J. Reichart, J. S. S. Damste, E. M. Crouch, and G. R. Dickens (2007), Environmental precursors to rapid light carbon injection at the Palaeocene/Eocene boundary, *Nature*, *450*(7173), 1218–1221.

Spero, H. J., J. Bijma, D. W. Lea, and B. E. Bemis (1997), Effect of seawater carbonate concentration on foraminiferal carbon and oxygen isotopes, *Nature*, *390*(6659), 497–500.

Spiro, B. (1991), Effects of minerals on Rock-Eval pyrolysis of kerogen, *J. Therm. Anal.*, *37*(7), 1513–1522.

Suan, G., E. Mattioli, B. Pittet, S. Mailliot, and C. Lécuyer (2008a), Evidence for major environmental perturbation prior to and during the Toarcian (Early Jurassic) oceanic anoxic event from the Lusitanian Basin, Portugal, *Paleoceanography*, *23*, PA1202, doi:10.1029/2007PA001459.

Suan, G., B. Pittet, I. Bour, E. Mattioli, L. V. Duarte, and S. Mailliot (2008b), Duration of the Early Toarcian carbon isotope excursion deduced from spectral analysis: Consequence for its possible causes, *Earth Planet. Sci. Lett.*, *267*(3–4), 666–679.

Suan, G., E. Mattioli, B. Pittet, C. Lécuyer, B. Suchéras-Marx, L. V. Duarte, M. Philippe, L. Reggiani, and F. Martineau (2010), Secular environmental precursors to Early Toarcian (Jurassic) extreme climate changes, *Earth Planet. Sci. Lett.*, *290*(3–4), 448–458.

Suan, G., et al. (2011), Polar record of Early Jurassic massive carbon injection, *Earth Planet. Sci. Lett.*, *312*(1–2), 102–113.

Suan, G., et al. (2013), Paleoenvironmental significance of Toarcian black shales and event deposits from southern Beaujolais, France, *Geol. Mag.*, *150*(4), 728–742.

Svensen, H., S. Planke, L. Chevallier, A. Malthe-Sørenssen, F. Corfu, and B. Jamtveit (2007), Hydrothermal venting of greenhouse gases triggering Early Jurassic global warming, *Earth Planet. Sci. Lett.*, *256*(3–4), 554–566.

Tyson, R. V. (1995), Bulk geochemical characterization and classification of organic matter: Stable carbon isotopes ($\delta^{13}C$), in *Sedimentary Organic Matter*, pp. 395–416, Springer, Netherlands.

Uchikawa, J., and R. E. Zeebe (2010), Examining possible effects of seawater pH decline on foraminiferal stable isotopes during the Paleocene-Eocene thermal maximum, *Paleoceanography*, *25*, PA2216, doi:10.1029/2009PA001864.

Ullmann, C. V., N. Thibault, M. Ruhl, S. P. Hesselbo, and C. Korte (2014), Effect of a Jurassic oceanic anoxic event on belemnite ecology and evolution, *Proc. Natl. Acad. Sci. U.S.A.*, *111*(28), 10,073–10,076.

van Breugel, Y., M. Baas, S. Schouten, E. Mattioli, and J. S. Sinninghe Damsté (2006), Isorenieratane record in black shales from the Paris Basin, France: Constraints on recycling of respired CO_2 as a mechanism for negative carbon isotope shifts during the Toarcian oceanic anoxic event, *Paleoceanography*, *21*, PA4220, doi:10.1029/2006PA001305.

van de Schootbrugge, B., J. M. McArthur, T. R. Bailey, Y. Rosenthal, J. D. Wright, and K. G. Miller (2005), Toarcian oceanic anoxic event: An assessment of global causes using belemnite C isotope records, *Paleoceanography*, *20*, PA3008, doi:10.1029/2004PA001102.

van de Schootbrugge, B., J. L. Payne, A. Tomasovych, J. Pross, J. Fiebig, M. Benbrahim, K. B. Föllmi, and T. M. Quan (2008), Carbon cycle perturbation and stabilization in the wake of the Triassic-Jurassic boundary mass-extinction event, *Geochem. Geophys. Geosyst.*, *9*, Q04028, doi:10.1029/2007GC001914.

van de Schootbrugge, B., A. Bachan, G. Suan, S. Richoz, and J. L. Payne (2013), Microbes, mud and methane: Cause and consequence of recurrent Early Jurassic anoxia following the end-Triassic mass extinction, *Palaeontology*, *56*, 685–709.